strongly depend on the number of ligand molecules on the metal (Table I). The rate constant for the dissociation of the glycinate ion from $[Ni(gly)_3]^-$ is independent of pH from pH 7 to 3.5 and becomes enhanced at pH <3.[25b] Similar dependence of k_{iL}^0 on the number of glycinate ions was observed for Ni(II)-gly$^-$ complexes[10,25] as shown in Table I.

Useful information can be obtained by comparing the rate constants. $k_{iL}^0/k_{(i-1)L}^0$ (=7-12) or $k_{iL}^H/k_{(i-1)L}^H$ (=33-40) for both Co(II)-gly$^-$ and Co(II)-acac$^-$ complexes are roughly constant with the exception of k_{3L}^0/k_{2L}^0 (=270) or k_{3L}^H/k_{2L}^H (=230) for the acetylacetonate system. k_{3L}^0/k_{2L}^0 or k_{3L}^H/k_{2L}^H for the acetylacetonate system is much larger than that for the glycinate system. It is also known that $[Co(acac)_2(H_2O)_2]$ in a solid state is a trans form.[26] These facts suggest that $[Co(acac)_2]$ is more stable than $[Co(gly)_2]$ against dissociation, and the geometry change of the $[Co(acac)_2]$ complexes upon dissociation might be important. $k_{iL}^0/k_{(i-1)L}^0$ (=12-16)[10b] and $k_{iL}^H/k_{(i-1)L}^H$ (=11-49)[25b] for Ni-gly$^-$ complex are similar to those of Co-gly$^-$ complex. However, k_{iL}^0 for the nickel complex is smaller than that for the cobalt complex by more than 2 orders of magnitude.

$k_{iL}^0(gly)/k_{iL}^0(en)$ depends little upon the number of ligand molecules on the metal ($k_{3L}^0(gly)/k_{3L}^0(en)$ = 6.2, $k_{2L}^0(gly)/k_{2L}^0(en)$ = 7.0, and $k_L^0(gly)/k_L^0(en)$ = 3.5), on the other hand, $k_{iL}^H(gly)/k_{iL}^H(en)$ depends significantly upon the number of the ligand molecules on the metal ($k_{3L}^H(gly)/k_{3L}^H(en)$ = 4.1, $k_{2L}^H(gly)/k_{2L}^H(en)$ = 0.58, and $k_L^H(gly)/k_L^H(en)$ = 0.066). This observation might be attributed to the fact that the total charge of the Co(II)-gly$^-$ complex changes in going from $[Co(gly)_3]^-$ to $[Co(gly)]^+$, which alters the ease of attack by proton, whereas the charge on Co(II)-en complexes is independent of the number of ligand. From the dissociation rate constants of $[Co(gly)_3]^-$ and $[Co(acac)_3]^-$, the following ratios of the rates were obtained: $k_{3L}^0(acac)/k_{3L}^0(gly)$ = 1.9, $k_{2L}^0(acac)/k_{2L}^0(gly)$ = 0.09, and $k_L^0(acac)/k_L^0(gly)$ = 0.06 for the acid-independent reactions and $k_{3L}^H(acac)/k_{3L}^H(gly)$ = 27, $k_{2L}^H(acac)/k_{2L}^H(gly)$ = 3.8, and $k_L^H(acac)/k_L^H(gly)$ = 3.6 for the acid-catalytic reactions. These results show that $k_{iL}^0(acac)$ is smaller than $k_{iL}^0(gly)$ by more than 1 order of magnitude with the exception of $k_{3L}^0(acac)$, and $k_{iL}^H(acac)$ is larger than $k_{iL}^H(gly)$. This observation indicates that the dissociation of acetylacetonate ion in $[Co(acac)_3]^-$ is more acid catalytic than that in $[Co(gly)_3]$. The mechanism suggested for the aquation reactions of the Co(II)-acac$^-$ complex is that the complex opens one end and the second end dissociates with the assistance of protons[8]. Although the mechanism is different from that of the Co(II)-gly$^-$ complex, the kinetic behavior of $[Co(acac)_3]^-$ is very similar to that of $[Co(gly)_3]^-$, indicating that the charge of the ligand more strongly influences kinetic behavior rather than the presence or absence of an attacking point for protons on the ligand.

Acknowledgment. We thank Prof. A. Henglein for supporting this work.

(26) Bullen, R. J. *Acta Crystallogr.* **1959**, *12*, 703.

Contribution from the Department of Chemistry,
York University, North York, Ontario, Canada M3J 1P3

Synthesis, Electrochemistry, and Kinetic Investigations of Low-Spin Ferrous Bis(difluoroboryl)bis(dioximate) Complexes[1,2]

David W. Thompson and Dennis V. Stynes*

Received November 27, 1989

The synthesis of new *trans*-$Fe(dioxBF_2)_2(CH_3CN)_2$ complexes (diox = dimethylglyoximate, naphthoquinone dioximate, benzoquinone dioximate) complexes and their conversion to a variety of $Fe(dioxBF_2)_2TL$ complexes (T or L = acetonitrile, 1-methylimidazole, pyridine, tributyl phosphite, tributylphosphine, *tert*-butyl isocyanide, tosylmethyl isocyanide, carbon monoxide) is described. These complexes display MLCT spectra and rate constants for axial ligation similar to those of the analogous $Fe(dioxH)_2TL$ complexes but have Fe(III/II) redox potentials 500 mV greater and ν_{CO} for the carbonyl derivatives some 60 cm^{-1} higher. Kinetic and equilibrium data for the CH_3CN derivatives obtained by spectrophotometric and flash-photolysis methods in acetonitrile solution and in toluene are compared with data for other FeN_4 systems.

Introduction

Extensive rate and equilibrium data for dissociative axial ligation reactions of complexes of the form *trans*-FeN_4TL (where N_4 is a planar tetradentate ligand such as bis(dioxime),[3] phthalocyanine,[4] or other macrocyclic ligand[5] and T and L are monodentate axial ligands such as imidazoles, pyridines, CO, RNC, PR_3, etc.) provide a rich source of quantitative information on metal-ligand bonding involving low-spin Fe(II). The neutral $Fe(dioxH)_2TL$ complexes (diox = dmg, npq, bqd) are soluble in noncoordinating solvents but generally have axial labilities orders of magnitude more inert than those of their heme counterparts.[3]

The availability of derivatives containing weaker axial ligands such as acetonitrile could significantly extend the chemistry of these systems. Such complexes may be useful in applications that require high lability and/or high binding constants such as CO scrubbing, catalysis, or possibly dioxygen binding.[6] While cationic $Fe(N_4)(CH_3CN)_2^{2+}$ derivatives are known for N_4 = Me_4[TIM],[7]

(1) Given in part at the 72nd Canadian Chemical Conference and Exhibition, University of Victoria, Victoria, British Columbia, Canada, June 4-8, 1989.

(2) Abbreviations: dmgH, dimethylglyoximate; $dmgBF_2$, (difluoroboryl)dimethylglyoximate; $dmgB(Ph)_2$, (diphenylboryl)dimethylglyoximate; bqdH, benzoquinone dioximate; $bqdBF_2$, (difluoroboryl)benzoquinone dioximate; npqH, naphthoquinone dioximate; $npqBF_2$, (difluoroboryl)-naphthoquinone dioximate; Me_4[TIM], 2,3,9,10-tetramethyl-1,2,8,11-tetraazacyclotetradeca-1,3,8,10-tetraene; Ph_4[TIM], 2,3,9,10-tetraphenyl-1,2,8,11-tetraazacyclotetradeca-1,3,8,10-tetraene; Pc, phthalocyanine; TPP, tetraphenylporphyrin; PpIX, protoporphyrin IX dimethyl ester; TAAB, tetrabenzo[*b,f,j,n*]-1,5,9,13-tetraazacyclohexadecane; [14]aneN$_4$, *meso*-5,5,7,12,12,14-hexamethyl-1,4,8,11-tetraazacyclotetradecane; MeIm, 1-methylimidazole; Im, imidazole; BuNC, *n*-butyl isocyanide; TMIC, (*p*-tolylsulfonyl)methyl isocyanide (tosylmethyl isocyanide); py, pyridine; CH_3CN, acetonitrile; $P(OBu)_3$, tributyl phosphite; MLCT, metal to ligand charge transfer. Rate constants are designated by k_{-L}^T for dissociation of the ligand L trans to T and by k_{+E}^T for addition of a ligand to the pentacoordinate intermediate trans to T. Equilibrium constants K_{LE}^T are for replacement of L by E trans to T. The shortened forms N (MeIm), PO ($P(OBu)_3$), and A (CH_3CN) are used as superscripts and subscripts.

(3) (a) Pomposo, F.; Stynes, D. V. *Inorg. Chem.* **1983**, *22*, 569. (b) Chen, X.; Stynes, D. V. *Inorg. Chem.* **1986**, *25*, 1173. (c) Siddiqui, N.; Stynes, D. V. *Inorg. Chem.* **1986**, *25*, 1982.

(4) (a) Stynes, D. V.; James, B. R. *J. Am. Chem. Soc.* **1974**, *96*, 2733. (b) Stynes, D. V. *J. Am. Chem. Soc.* **1974**, *96*, 5942. (c) Stynes, D. V. *Inorg. Chem.* **1977**, *16*, 1170. (d) Martinsen, J.; Miller, M.; Trojan, D.; Sweigart, D. A. *Inorg. Chem.* **1980**, *19*, 2162.

(5) (a) Stynes, D. V.; Hui, Y. S.; Chew, V. *Inorg. Chem.* **1982**, *21*, 1222. (b) Kildahl, N. K.; Lewis, T. J.; Antonopoulos, C. *Inorg. Chem.* **1981**, *20*, 3952. (c) Kildahl, N. K.; Balkus, K. J., Jr.; Flynn, M. *Inorg. Chem.* **1983**, *22*, 589. (d) Kildahl, N. K.; Antonopoulos, G.; Fortier, N. E.; Hobey, W. D. *Inorg. Chem.* **1985**, *24*, 429. (e) Butler, A.; Linck, R. G. *Inorg. Chem.* **1984**, *23*, 2227. (f) Butler, A.; Linck, R. G. *Inorg. Chem.* **1984**, *23*, 4545. (g) Pang, I. W.; Stynes, D. V. *Inorg. Chem.* **1977**, *16*, 2192. (h) Stynes, D. V.; Singh, K.; Ng, B.; Wilshire, S. *Inorg. Chim. Acta* **1982**, *58*, 179.

(6) (a) Koval, C. A.; Noble, R. D.; Way, J. D.; Louie, B.; Reyes, Z. E.; Bateman, B. R.; Horn, G. M.; Reed, D. L. *Inorg. Chem.* **1985**, *24*, 1147. (b) Reichgott, D. W.; Rose, N. J. *J. Am. Chem. Soc.* **1977**, *99*, 1813.

0020-1669/90/1329-3815$02.50/0

[14]aneN$_4$, [15]aneN$_4$,[5a,8] and TAAB,[9,5g] no neutral *trans*-Fe(dioxH)$_2$(CH$_3$CN)$_2$ complexes have been previously characterized. Attempts to obtain Fe(dioxH)$_2$(CH$_3$CN)$_2$ complexes in our lab by direct methods have not been successful. However, the well-known reaction of metal dioximates with BF$_3$·Et$_2$O,[10-12] affords a convenient route to acetonitrile complexes of Fe(dioxBF$_2$)$_2$(CH$_3$CN)$_2$. The only previous studies of reactions of iron dimethylglyoximate with BF$_3$·Et$_2$O resulted in the formation of inert tris clathrochelates of the form Fe(dmg)$_3$(BF)$_2$.[13] We report here a variety of new labile Fe(dioxBF$_2$)$_2$TL complexes, including the highly labile bis(acetonitrile) species, of the three dioximes shown as

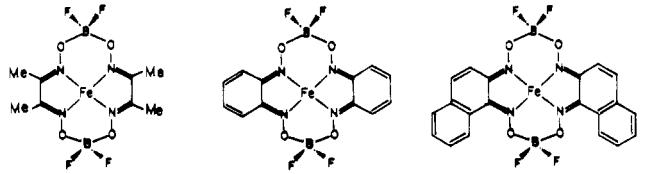

Results of the electrochemical, spectroscopic, and kinetic studies on these systems are compared with those for the Fe(dioxH)$_2$TL analogues.

Experimental Section

Materials. The complexes Fe(dmgH)$_2$(py)$_2$, Fe(dmgH)$_2$(py)CO, Fe(npqH)$_2$(py)$_2$, and Fe(bqdH)$_2$(py)$_2$ were prepared by published procedures.[3] Ferrous acetate was prepared from iron powder (325 mesh) and glacial acetic acid and stored under nitrogen.[3] The benzoquinone dioxime (bqdH$_2$) ligand was synthesized by borohydride reduction of benzofuroxan.[14] Toluene was distilled from LiAlH$_4$. All other ligands and solvents were from standard sources and were used as received except where otherwise noted.

Physical Measurements. An Aminco DW-2a UV/vis spectrophotometer was used to record visible spectra. NMR spectra were obtained on a Varian EM-360 or a Bruker AM300 instrument with an Aspec 3000 computer, using CDCl$_3$ or CD$_3$CN as the solvents and TMS as an internal standard. Infrared spectra were obtained on a Nicolet 20 SX FTIR instrument in KBr disks. Elemental analyses were performed by Canadian Microanalytical Service Ltd., Vancouver, BC, Canada.

Electrochemical measurements were performed by using a three-electrode PAR Model 173 potentiostat/galvanostat equipped with a PAR 175 universal programmer. The cyclic voltammograms were recorded on a PAR Model 200A X-Y recorder. Measurements were performed in CH$_3$CN with 0.1 M TEAP (Eastman Kodak) as the supporting electrolyte. Electrochemical measurements in nonaqueous solvents were measured relative to the internal standard, the ferrocenium/ferrocene (Fc$^+$/Fc) redox couple (0.40 V vs SCE, ΔE_p = 80–90 mV), as per the IUPAC recommendations.[15] A two-compartment cell was employed where the reference electrode was separated from the counter and working electrodes by a medium-porosity glass frit. Prior to electrochemical measurements, the solutions were deoxygenated with a vigorous N$_2$ purge for 10–15 min. The $E_{1/2}$ values were determined by employing the formula $E_{1/2} = (E_{pa} + E_{pc})/2$, where E_{pa} and E_{pc} are the anodic and cathodic peak potentials, respectively. In order to minimize the effect that changing the scan rate has on quasi-reversible systems, all half-wave potentials were reported for scan rates of 200 mV s^{-1}.

Syntheses. All syntheses were carried out under a nitrogen atmosphere and in N$_2$-purged solvents unless otherwise indicated.

Fe(dmgBF$_2$)$_2$(py)(CO). To 100 mL of CO-saturated CH$_2$Cl$_2$ was added Fe(dmgH)$_2$(py)(CO) (8 g, 20 mmol), and the solution was cooled to 0 °C. Under a CO purge with rapid stirring, 11 mL of BF$_3$·Et$_2$O (90 mmol) was added over a period of 5 min. After the solution was stirred for 45 min at 0 °C, 20 mL of absolute EtOH was added, and the volume was reduced to 20 mL in vacuo. The product was filtered out, washed twice with 10 mL of ice-cold EtOH, and dried in vacuo (yield 5.4 g, 55%). NMR (CDCl$_3$): δ 2.33 (dmgBF$_2$, CH$_3$), 7.33, 7.74, 8.49 (py, C–H). IR: 2049 (ν_{CO}), 1174 cm^{-1} (ν_{BO}).

Fe(dmgBF$_2$)$_2$(py)$_2$. Method A. A solution of 2.2 g of Fe(dmgBF$_2$)$_2$(py)(CO) (4.5 mmol) in 50 mL of CHCl$_3$ containing 5 mL of pyridine (62 mmol) was refluxed for 2 h, affording a precipitate of Fe(dmgBF$_2$)$_2$(py)$_2$. The product was filtered out, washed with petroleum ether (40–60 °C), and dried in vacuo (yield 2 g, 83%). Anal. Calcd for FeC$_{18}$H$_{22}$B$_2$F$_4$N$_6$O$_4$: C, 40.06; H, 4.08; N, 15.58. Found: C, 38.91; H, 3.97; N, 14.51. NMR (CDCl$_3$): δ 2.66 (dmgBF$_2$, CH$_3$), 6.98, 7.48, 7.74 (py, C–H). Visible: $\epsilon = 8.9 \times 10^3$ M^{-1} cm^{-1} at λ = 518 nm.

Method B. BF$_3$·Et$_2$O (14 mL, 0.11 mol) was added over a period of 1 min to a suspension of Fe(dmgH)$_2$(py)$_2$ (10 g, 23 mmol) in 100 mL of anhydrous diethyl ether containing 30 mL of CH$_3$CN. During the course of the BF$_3$·Et$_2$O addition, the red solution turns to golden yellow and a precipitate of the Fe(dmgBF$_2$)$_2$(CH$_3$CN)$_2$ complex is observed. The precipitate was filtered out and converted to the Fe(dmgBF$_2$)$_2$(py)$_2$ complex by addition of 100 mL of CHCl$_3$ containing 10 mL of pyridine (0.12 mol). The volume was reduced to 20 mL and the precipitate filtered out, washed with petroleum ether (40–60 °C), and dried in vacuo. The product was recrystallized by adding 1.2 g of the Fe(dmgBF$_2$)$_2$(py)$_2$ complex to 50 mL of hot CH$_2$Cl$_2$, filtering the mixture, and allowing the solution to cool overnight (yield 0.7 g, 58%).

Fe(dmgBF$_2$)$_2$(CH$_3$CN)$_2$. Attempts to isolate the Fe(dmgBF$_2$)$_2$(CH$_3$CN)$_2$ complex formed during the synthesis outlined in method B of the Fe(dmgBF$_2$)$_2$(py)$_2$ synthesis were unsuccessful because the bis(acetonitrile) complex reacted in the solid state to yield Fe(dmg)$_3$(BF)$_2$. The following method proved convenient. To a rapidly stirred suspension of Fe(dmgBF$_2$)$_2$(py)$_2$ (0.3 g, 0.5 mmol) in 20 mL of CH$_3$CN was added 15 mL of 0.1 M aqueous HCl (15 mmol). An orange yellow precipitate formed immediately. The product was filtered out, washed with H$_2$O containing 5% CH$_3$CN and 5% 0.1 M HCl (v/v), and dried in vacuo (yield 0.27 g, 85%). Anal. Calcd for FeC$_{12}$H$_{18}$B$_2$F$_4$N$_6$O$_4$: C, 31.09; H, 3.88; N, 18.13. Found: C, 30.65; H, 3.85; N, 17.68. NMR (95% CDCl$_3$/CD$_3$CN): δ 2.00 (CH$_3$CN, CH$_3$), 2.55 (dmgBF$_2$, CH$_3$). Visible: $\epsilon = 7.7 \times 10^3$ M^{-1} cm^{-1} at λ = 445 nm.

Fe(dmgBF$_2$)(CH$_3$CN)(CO). Solid Fe(dmgBF$_2$)$_2$(CH$_3$CN)$_2$ (0.7 g, 1.5 mmol) was added to 40 mL of CO-saturated CH$_2$Cl$_2$. This mixture was warmed to reflux under CO and the volume reduced until a light yellow crystalline solid was observed. Hexane (25–35 mL, CO saturated) was slowly added and the solution cooled to yield a light yellow crystalline material. The precipitate was filtered out, washed with petroleum ether (40–60 °C), and dried in vacuo 0.66 g, 95%). Anal. Calcd for FeC$_{11}$H$_{15}$B$_2$F$_4$N$_5$O$_5$: C, 29.32; H, 3.33; N, 15.55. Found: C, 27.64, H, 3.25, N, 14.52. NMR (CO-saturated CDCl$_3$): δ 2.18 (CH$_3$CN, CH$_3$), 2.47 (dmgBF$_2$, CH$_3$). Visible: $\epsilon = 4.5 \times 10^3$ M^{-1} cm^{-1} at λ = 370 nm.

Fe(dioxBF$_2$)$_2$(CH$_3$CN)(RNC). A small amount of Fe(dioxBF$_2$)$_2$(CH$_3$CN)$_2$ (200 mg) was added to a mixture of 1 mL of CH$_3$CN, 5 mL of CH$_2$CL$_2$, and a slight excess of RNC (TMIC or BuNC). The solution was stirred for maximum of 2 min, and hexane (20 mL) was added to induce precipitation. The solution was filtered and the product dried in vacuo (yield 60–70%). All NMR spectra were run in CDCl$_3$. NMR for Fe(dmgBF$_2$)$_2$(CH$_3$CN)(BuNC): δ 0.84, 1.25, 1.38, 3.39 (BuNC, CH), 2.06 (CH$_3$CN, CH$_3$), 2.46 (dmgBF$_2$, CH$_3$). NMR for Fe(dmgBF$_2$)$_2$(CH$_3$CN)(TMIC): δ 2.12 (CH$_3$CN, CH$_3$), 2.45 (dmgBF$_2$, CH$_3$), 4.44 (TMIC, CH$_2$), 7.4–7.8 (TMIC, CH). NMR for Fe(NpqBF$_2$)$_2$(CH$_3$CN)(BuNC): δ 0.60, 1.25, 1.38. 3.30 (BuNC, CH), 2.00 (CH$_3$CN, CH$_3$), 7.02–7.53, 9.62, 9.64 (npqBF$_2$, CH).

Fe(dmgB(C$_6$H$_5$)$_2$)$_2$(MeIm)$_2$. A solution of 50 mL of CHCl$_3$, Fe(dmgH)$_2$(MeIm)$_2$ (0.5 g, 0.9 mmol), and B(C$_6$H$_5$)$_2$(NH$_2$CH$_2$O) (0.6 g, 2.7 mmol) was refluxed under CO for 10 h. The CO was discontinued, toluene added, and the CHCl$_3$ driven off. The toluene solution was refluxed for 40 h at 110 °C. Cooling and filtration yielded 0.4 g of an impure brown solid. The brown product (0.1 g) was heated in CHCl$_3$ with a few drops of MeIm. Addition of petroleum ether gave a pink crystalline precipitate. NMR (CDCl$_3$): δ 2.48 (dmgB(C$_6$H$_5$)$_2$, CH$_3$), 3.17 (MeIm, CH$_3$), 7–7.5 (broad, B(C$_6$H$_5$), CH). IR: 1198 cm^{-1} (ν_{BO}). UV/vis: λ_{max} 405 nm.

(7) Baldwin, D. A.; Pfieffer, R. M.; Reichgott, D. W.; Rose, N. J. *J. Am. Chem. Soc.* **1973**, *95*, 5152.
(8) Watkins, D. D.; Riley, D. P.; Stone, J. A.; Busch, D. H. *Inorg. Chem.* **1976**, *15*, 387.
(9) Melson, G. A.; Busch, D. H. *J. Am. Chem. Soc.* **1964**, *88*, 4834.
(10) Schrauzer, G. N. *Chem. Ber.* **1962**, *95*, 1438.
(11) (a) Schrauzer, G. N.; Windgassen, R. J. *J. Am. Chem. Soc.* **1966**, *88*, 3738. (b) Magnuson, J. E.; Weber, J. H. *J. Organomet. Chem.* **1974**, *74*, 135. (c) Ramanujam, V. V.; Alexander, V. *Inorg. Chem.* **1987**, *26*, 3124. (d) Bakac, A.; Espenson, J. H. *J. Am. Chem. Soc.* **1984**, *106*, 5197. (e) Bakac, A.; Brynildson, M. E.; Espenson, J. H. *Inorg. Chem.* **1986**, *25*, 4108.
(12) (a) Gagne, R. R.; Allison, J. L.; Lisensky, G. C. *Inorg. Chem.* **1978**, *17*, 3563. (b) Gagne, R. R.; Allison, J. L.; Ingle, G. A. *Inorg. Chem.* **1979**, *18*, 2767.
(13) Jackels, S. C.; Rose, N. J. *Inorg. Chem.* **1973**, *12*, 1232.
(14) (a) Smith, P. A.; Boyer, J. H. *Org. Synth.* **1951**, *31*, 14. (b) Boyer, J. H.; Ellzey, S. E., Jr. *J. Am. Chem. Soc.* **1960**, *82*, 2525.
(15) (a) Gritzer, G.; Kuta, J. *Pure Appl. Chem.* **1982**, *54*, 1528. (b) Gagne, R. R.; Koval, C. A.; Lisensky, G. C. *Inorg. Chem.* **1980**, *19*, 2854.
(16) Brown, E. R.; Large, R. F. In *Physical Methods of Chemistry, Part IIA: Electrochemical Methods*; Weissberger, A., Rossiter, B. W., Eds.; 1971; Chapter 6.

$Fe(npqBF_2)_2(CH_3CN)_2$. Dropwise addition of $BF_3{\cdot}Et_2O$ (5.5 mL, 44 mmol) over a period of 5 min to a rapidly stirred solution of $Fe(npqH)_2(py)_2$ (5 g, 8.5 mmol) in 40 mL of CH_3CN resulted in a green solution that slowly turned purple. Precipitation of the complex was induced by addition of 40 mL of 0.1 M aqueous HCl. Filtration, followed by washing twice with 50% (v/v) CH_3CN/0.1 M HCl(aq) and drying in vacuo, yielded 4.7 g of the complex (yield 90%). NMR (CD_3CN): δ 2.00 (CH_3CN, CH_3), 7.19–7.96, 9.54–9.56 ($npqBF_2$, CH). Visible: $\epsilon = 2.2 \times 10^4$ M^{-1} cm^{-1} at $\lambda = 570$ nm.

$Fe(npqBF_2)_2(CH_3CN)(CO)$. A solution of $Fe(npqBF_2)_2(CH_3CN)_2$ (1 g, 1.7 mmol) in 15 mL of $CHCl_3$ containing 5 mL of CH_3CN was stirred at room temperature under CO flow for 20 min. After addition of 100 mL of CO-saturated hexane, the solution was then placed in a freezer for 2 h. The precipitate was filtered out, washed with hexane, and dried in vacuo (yield 0.57 g, 56%). NMR (CO-saturated $CDCl_3$): δ 2.08 (CH_3CN, CH_3), 7.06–7.09, 7.46–7.61, 9.52, 9.58 ($npqBF_2$, CH). IR: 2062 cm^{-1} (ν_{CO}).

$Fe(npqBF_2)_2(MeIm)_2$. Solid $Fe(npqBF_2)_2(CH_3CN)_2$ (0.5 g, 0.8 mmol) was added to 50 mL of $CHCl_3$ containing 0.4 mL of MeIm (5.0 mmol). The dark green solution was filtered and concentrated to 15 mL with gentle heating and hexane was added. The product was filtered out, washed with ether, and dried in vacuo. (yield 0.46 g, 79.8%) NMR ($CDCl_3$): δ 3.37 (MeIm, CH_3), 6.41, 6.99 (MeIm, CH), 7.50–7.69, 9.74, 9.77 ($npqBF_2$, CH).

$Fe(npqBF_2)_2(py)_2$ was obtained similarly to the procedure outlined for the $Fe(npqBF_2)_2(MeIm)_2$ complex.

$Fe(bqdBF_2)_2(CH_3CN)_2$. A suspension of $Fe(OAc)_2{\cdot}4H_2O$ (0.49 g, 2.3 mmol) in 20 mL of diethyl ether containing 10 mL of CH_3CN was stirred for 5 min while 2 mL of $BF_3{\cdot}Et_2O$ (0.16 mol) was added. The $bqdH_2$ ligand (0.5 g, 3.6 mmol) was added under a vigorous N_2 purge, and the reactants were stirred for 20 min. Filtration, followed by washing with three 10-mL aliquots of ice-cold ether and drying in vacuo, yielded 0.38 g of the complex (yield 42%). NMR ($CDCl_3$/0.01 M CD_3CN): δ 6.75–6.78, 7.56–7.59 ($bqdBF_2$, CH). Visible: $\epsilon = 1.8 \times 10^4$ M^{-1} cm^{-1} at $\lambda = 596$ nm.

Kinetics. All reactions were routinely run in serum-capped nitrogen-purged cuvettes (or CO purging for reactions with CO) and monitored by visible spectroscopy. Temperature control was maintained by water circulation through a thermostatable cell holder. The temperature of the cell holder was read from an RTD device that was attached to the cell holder. Reaction solutions were prepared either by injecting 10–100 μL of ligand (either neat or as a toluene solution) into a 1-cm cuvette containing the complex or, conversely, by injecting concentrated solutions of the complex into cuvettes containing the ligand. Concentrations of the complexes employed were typically 10^{-4} M. Rate constant were derived from a linear least-squares fit of log $[(A - A_\infty)/(A_0 - A_\infty)]$ vs time by using a microcomputer analysis described elsewhere.[3]

Flash Photolysis. An Applied Photophysics flash-photolysis apparatus incorporating two Nobellight xenon flash lamps mounted in a cylindrical flash cavity was used with typical discharge energies from 15 to 20 kV. The flash profile had a width of 15 μs and decays with a rate constant of 8×10^4 s^{-1}. The voltage vs time trace was recorded and digitized by a Tektronix Model 2430A digital oscilloscope. A microcomputer was used to obtain absorbance vs time data and do first-order kinetic analysis. As required, a Yvon-Jobin Model 5/123 V grating monochromator or cutoff filters were mounted between the monitoring beam and the flash cavity to reduce complications associated with photolysis by the monitoring light. Nitrogen- or CO-purged solutions in 10 cm path length Pyrex cells with typical absorbances of 1.0–2.0 at the absorbance maximum of the reactant were thermostated for 10 min prior to flashing, and the visible spectrum was monitored before and after each experiment on a spectrophotometer. Typical absorbance changes for carbonyl photolyses were 0.1–0.8 absorbance units.

Reactions with CO in acetonitrile were obtained in several cases by conventional mixing methods and via the flash method and gave identical results. The faster reactions in toluene were studied exclusively by the flash-photolysis method.

A trapping method was routinely used to investigate the more rapid reactions involving py and TMIC. A sample of $Fe(dioxBF_2)_2(T)CO$ (T = py, CH_3CN) was photolyzed in the presence of excess CH_3CN and entering ligand E (E = CO, py, TMIC). Under the conditions of the experiments ($[CH_3CN] \gg [py]$) the pentacoordinate $Fe(dioxBF_2)_2T$ is trapped efficiently as the $Fe(dioxBF_2)_2(T)(CH_3CN)$ complex. The fate of $Fe(dioxBF_2)_2(T)(CH_3CN)$ is monitored with time as a function of [E].

Results

Synthesis. The new $Fe(dioxBF_2)_2(CH_3CN)_2$ complexes have been obtained as crystalline solids and have been characterized by visible spectroscopy, NMR spectroscopy, and elemental analysis. The direct reaction of excess $BF_3{\cdot}Et_2O$ with the $Fe(dioxH)_2(py)_2$ complexes in acetonitrile solution readily affords the $Fe(npqBF_2)_2(CH_3CN)_2$ and $Fe(bqdBF_2)_2(CH_3CN)_2$ complexes (eq 1). However, $Fe(dmgH)_2(py)_2$ reacts with $BF_3{\cdot}Et_2O$

$$Fe(dioxH)_2(py)_2 + 4BF_3 + 2CH_3CN \rightarrow Fe(dioxBF_2)_2(CH_3CN)_2 + 2HF + 2pyBF_3 \quad (1)$$

to give a product whose visible spectrum, NMR spectrum, and general lack of reactivity show it to be identical with $Fe(dmg)_3(BF)_2$ complex previously reported by Rose.[13] It was clear that the conversion of the $Fe(dmgH)_2(py)_2$ to the clathrochelate required pyridine dissociation as well as some decomposition to provide the third dmg ligand. The conversion to the $Fe(dmg)_3(BF)_2$ complex was suppressed by carrying out the $BF_3{\cdot}Et_2O$ treatment on the substitution-inert $Fe(dmgH)_2(py)CO$ complex. The following reaction sequence proved convenient:

$$Fe(dmgH)_2(py)CO + 2BF_3{\cdot}Et_2O \rightarrow Fe(dmgBF_2)_2(py)CO + 2HF + 2Et_2O \xrightarrow{[py]} Fe(dmgBF_2)_2(py)_2 + CO \quad (2)$$

Subsequent treatment of the labile $Fe(dmgBF_2)_2(py)_2$ species with aqueous HCl in acetonitrile gave the desired $Fe(dmgBF_2)_2(CH_3CN)_2$ complex via eq 3. A variety of axially ligated species

$$2CH_3CN + Fe(dmgBF_2)_2(py)_2 + 2HCl \rightarrow Fe(dmgBF_2)_2(CH_3CN)_2 + 2py{\cdot}HCl \quad (3)$$

are easily obtained (Table I). The more inert $Fe(dmgBF_2)_2L_2$ species are quite stable in solution or as solids. However, solid samples of the $Fe(dmgBF_2)_2(CH_3CN)_2$ complex slowly became contaminated with the $Fe(dmg)_3(BF)_2$ complex, possibly initiated by hydrolysis of the BF bond.

Bis(diphenylboryl)bis(dioximate) compounds can also be obtained by reaction of the $Fe(dmgH)_2$ complexes with diphenylboron–ethanolamine adduct. These materials were found to be similar to the BF_2-substituted complexes and were not investigated further.

Table I. Visible Spectral Data for $Fe(dioxBF_2)_2TL$ Complexes: λ_{max} (nm) in Acetonitrile Solution

T	L	$dmgBF_2$	$npqBF_2$	$bqdBF_2$[b]
CH_3CN	CH_3CN	445	568	596
	py	480	617	656
	MeIm	480	630	
	PBu_3	483	606	
	$P(OBu)_3$	454	569	580
	BuNC	430	540	560
	TMIC	419	526	539
	CO	350–370	470	465
MeIm	MeIm	533	683	716
	PBu_3	505	639	
	BuNC	457	584	
	TMIC	439	560	584
	CO	404	494	
py	py	518[a]	656	687
	$P(OBu)_3$	475	539	
	CO	404	495	501
PBu_3	PBu_3	491	606	617
$P(OBu)_3$	$P(OBu)_3$	431	539	540
BuNC	BuNC	414	516	525
TMIC	TMIC	392	492	500

[a] Two additional bands assigned as Fe–py MLCT at 364 and 403 nm. [b] Additional bands assigned to intraligand transitions are typically observed between 380 and 400 nm. The positions of these bands are independent of changes in the axial ligands.

Spectral Features. The visible spectra of the ferrous bis(dioximate) complexes are dominated by an intense band assigned to a metal d(xz,yz) to oxime π^* charge transfer (MLCT). The

Table II. IR Data[a] for $FeN_4T(CO)$ Complexes

complex	T	ν_{CO}, cm^{-1}
$Fe(dmgH)_2$[b]	py	1985
$Fe(dmgH)_2$[b]	MeIm	1978
$Fe(dmgB(Ph)_2)_2$	MeIm	2038
$Fe(dmgBF_2)_2$	py	2049
$Fe(dmgBF_2)_2$	CH_3CN	2048
$Fe(npqH)_2$[b]	py	2010
$Fe(npqBF_2)_2$	py	2062
$Fe(npqBF_2)_2$	CH_3CN	2062
$Fe(bqdH)_2$	MeIm	2028
$Fe(bqdBF_2)_2$	CH_3CN	2063
$Fe(Me_4[TIM])^{2+}$[c]	MeIm	2030
$Fe(Me_4[TIM])^{2+}$[c]	CH_3CN	2029
$Fe(TAAB)^{2+}$[c]	CH_3CN	2038
$Fe([14]aneN_4)^{2+}$[c]	CH_3CN	1985

[a] KBr disk. [b] Reference 3c. [c] Reference 5a.

dependence of the MLCT band on axial ligands (Table I) and specific oxime has been described previously.[3] While the MLCT bands of the $Fe(dioxBF_2)_2TL$ species are similar to those of the corresponding $Fe(dioxH)_2TL$ complexes, they are not identical. In addition a band at 417 nm assigned to metal to pyridine charge transfer[3] in the $Fe(dmgH)_2(py)_2$ complex is split into two bands at 364 and 403 nm in the $Fe(dmgBF_2)_2(py)_2$ complex (Figure 3). These distinctive spectral differences allow the routine distinction between the $Fe(dioxH)_2$ and the $Fe(dioxBF_2)_2$ complexes. For $Fe(bqdBF_2)_2TL$ and $Fe(npqBF_2)_2TL$ complexes, intraligand oxime bands occurring typically between 380 and 400 nm are found 20 nm lower than those of the dioxH analogues. These distinctions in visible spectra are retained throughout ligand substitution reactions, indicating that the BF_2 groups remain intact under reaction conditions.

The $Fe(dioxBF_2)_2(T)CO$ complexes have values for ν_{CO} that are dramatically greater than those for the analogous $Fe(dioxH)_2(T)CO$ complexes. Carbon monoxide stretching frequencies for a wide variety of Fe(II) macrocycles given in Table II range from 1970 to 2060 cm^{-1}. The BF_2 derivatives have some of the highest stretching frequencies for FeN_4 systems studied to date.[17] The trends in ν_{CO} with oxime parallel those previously reported for the $Fe(dioxH)_2$ systems (dmg < npq < bqd).

Electrochemical Data. The reduction potentials of the $Fe(N_4)TL$ complexes were measured by cyclic voltammetry in acetonitrile solution (Table III). Peak separations greater than 59 mV suggest that the electrode reactions are at best quasi-reversible.[16]

The potentials in Table III show that $E_{1/2}$ is increased by BF_2 substitution, by the presence of axial π-acceptor ligands (MeIm < py < CH_3CN < BuNC < TMIC < CO) and by the nature of the dioxime ($dmgBF_2 \ll npqBF_2 < bqdBF_2$). The BF_2 substituent causes a shift in $Fe(diox)_2$ potentials, which places them close to the values found for +2-charged $FeTIM^{2+}$ systems. The much higher potentials account for the substantially greater air stability of BF_2 derivatives of all three diox systems.

Reactions in Acetonitrile. The kinetics of ligand substitution reactions of the $Fe(dioxBF_2)_2(CH_3CN)_2$ and $Fe(Me_4[TIM])(CH_3CN)_2^{2+}$ complexes were investigated for entering ligands CO, TMIC, BuNC, $P(OBu)_3$, and py. The reaction with CO proceeds according to eq 4. For the other ligands investigated two distinct steps are observed giving the mono- and disubstituted product (eqs 5 and 6).

$$FeN_4(CH_3CN)_2 + CO \rightarrow FeN_4(CH_3CN)(CO) + CH_3CN \quad (4)$$

$$FeN_4(CH_3CN)_2 + E \rightarrow FeN_4(CH_3CN)E + CH_3CN \quad (5)$$

$$FeN_4(CH_3CN)E + E \rightarrow FeN_4E_2 + CH_3CN \quad (6)$$

(17) Goedken, V. L. In *Coordination Chemistry of Macrocyclic Compounds*; Melson, D. A., Eds.; Plenum Press: New York, 1979; Chapter 10.

Table III. $E_{1/2}$[a] for $FeN_4TL^{n+/(n-1)+}$ Complexes in CH_3CN (0.1 M TEAP)

	$E_{1/2}$, V vs Fc^+/Fc	ΔE_p, mV
$Fe(dmgH)_2(MeIm)_2^{+/0}$	−0.48	70
$Fe(dmgBF_2)_2(MeIm)_2^{+/0}$	0.06	90
$Fe(dmgBF_2)_2(py)_2^{+/0}$	0.36	100
$Fe(dmgBF_2)_2(CH_3CN)_2^{+/0}$	0.55	85
$Fe(dmgBF_2)_2(CH_3CN)(BuNC)^{+/0}$	0.65	92
$Fe(dmgBF_2)_2(CH_3CN)(TMIC)^{+/0}$	0.76	130
$Fe(dmgBF_2)_2(CH_3CN)CO^{+/0}$	1.2[b]	irr
$Fe(npqBF_2)_2(MeIm)_2^{+/0}$	0.24	140
$Fe(npqBF_2)_2(CH_3CN)_2^{+/0}$	0.62	90
$Fe(npqBF_2)_2(CH_3CN)(TMIC)^{+/0}$	0.85[b]	irr
$Fe(bqdBF_2)_2(MeIm)_2^{+/0}$	0.27	95
$Fe(Me_4[TIM])(MeIm)_2^{3+/2+}$	0.15[c]	
$Fe(Me_4[TIM])(CH_3CN)_2^{3+/2+}$	0.56[c,d]	72
$Fe(Me_4[TIM])(CH_3CN)(TMIC)^{3+/2+}$	0.83	200
$Fe(Ph_4[TIM])(MeIm)_2^{3+/2+}$	0.45[c]	
$Fe(Ph_4[TIM])(CH_3CN)_2^{3+/2+}$	0.85[c]	
$Fe(TPP)(Im)_2^{+/0}$	−0.51[e]	
$Fe(TPP)(py)_2^{+/0}$	−0.37[e]	

[a] $E_{1/2} = (E_{pa} + E_{pc})/2$; redox processes assigned to Fe(III/II) reduction. [b] Irreversible, no return wave; anodic potential is reported. [c] Reference 5d, referenced vs Fc^+/Fc. [d] Repeated in this work, referenced vs Fc^+/Fc, in excellent agreement with the result of Kildahl.[5d] [e] Felton, R. H. In *The Porphyrins*; Vol. V, Dolphin, D., Ed.; Academic: New York, 1978; Vol. V. Referenced versus Fc^+/Fc.

Table IV. Kinetic and Equilibrium Data for CO[a] Binding to $FeN_4(CH_3CN)_2$ Complexes in Acetonitrile (T = 25 °C) according to

$$FeN_4(CH_3CN)_2 + CO \underset{k_{+A}^A}{\overset{k_{-A}^A}{\rightleftharpoons}} FeN_4(CH_3CN) \underset{k_{-CO}^A}{\overset{k_{+CO}^A}{\rightleftharpoons}} FeN_4(CH_3CN)CO + CH_3CN$$

N_4	$10^3 k_{-CO}^A$, s^{-1}	$k_{-A}^A(k_{+CO}^A/k_{+A}^A)$, s^{-1}	$10^{-3}K_{A,CO}^A$
$dmgBF_2$	0.15 (0.007)	52 (3)	350 (40)
$bqdBF_2$	42 (5)	186 (6)	4.4 (0.6)
$npqBF_2$	4.3 (0.2)	34 (3)	7.9 (1.0)
$Me_4[TIM]$	0.49 (0.05)[b]	5.9 (0.5)	13 (2)
$[14]aneN_4$[c]	0.77	5.0[d]	6.5
$TAAB^{2+}$			0.086[c]

[a] A solubility of CO in acetonitrile of 9×10^{-3} M is assumed, similar to that reported for propionitrile: Gjaldbaek, J. C.; Andersen, E. K. *Acta Chem. Scand.* **1954**, *8*, 1398. [b] Within experimental error of 4.3 $\times 10^{-3}$ s^{-1} previously determined.[5a] [c] From data in ref 5a. [d] $k_{-A}^A(k_{+CO}^A/k_{+A}^A)$ calculated by $K_{A,CO}^A/k_{-CO}^A$.

Assuming a dissociative mechanism, the pseudo-first-order rate constant for each step is given by eq 7, which simplifies to eq 8 since the solvent is CH_3CN.

$$k_{obs} = (k_{-A}^A k_{+E}^A[E] + k_{-E}^A k_{+A}^A[CH_3CN])/(k_{+A}^A[CH_3CN] + k_{+E}^A[E]) \quad (7)$$

$$k_{obs} = k_{-A}^A k_{+E}^A[E]/k_{+A}^A[CH_3CN] + k_{-E}^A \quad (8)$$

Plots of k_{obs} vs [E] were linear, affording the rate constants given in Table IV. Typical plots for the reaction with CO are given in Figure 1. The lines for npq and bqd systems give nonzero intercepts from which the dissociation rate for CO is obtained. For the dmg system the intercept is too small to give a reliable value for k_{-CO}^A. The rate constants k_{-CO}^A were independently obtained from the rate of the reaction of the carbonyl complex with MeIm in eq 9, whose rate-determining step under the conditions of the experiment was shown to be loss of CO trans to CH_3CN.[18] The equilibrium constant for eq 4, $K_{A,CO}^A$, is obtained

$$FeN_4(CH_3CN)(CO) + MeIm \rightarrow FeN_4(MeIm)_2 + CH_3CN + CO \quad (9)$$

Table V. Kinetic Data[a] for $FeN_4(CH_3CN)_2$ Complexes in CH_3CN at 25 °C

$$FeN_4(CH_3CN)_2 + E \rightarrow FeN_4(CH_3CN)E + CH_3CN$$

	$k_{-A}^{A}(k_{+E}^{A}/k_{+A}^{A})$, s^{-1} N_4			
E	$dmgBF_2$	$npqBF_2$	$bqdBF_2$	$Me_4[TIM]$
CO	52 (3)	34 (2.5)	186 (6)	5.9 (0.5)
$P(OBu)_3$	190 (21)	410 (20)	4100 (200)	*b*
TMiC	4400 (400)	470 (40)	7850 (440)	110 (15)
BuNC	8400 (1000)	920 (15)	$>10^4$	130 (10)
py	7700 (400)	1180 (100)		

$$FeN_4(CH_3CN)E + E \rightarrow FeN_4(E)_2 + CH_3CN$$

	$10^2k_{-A}^{E}(k_{+E}^{E}/k_{+A}^{E})$, s^{-1} N_4		
	$dmgBF_2$	$npqBF_2$	$bqdBF_2$
$P(OBu)_3$	3 (0.2)	3 (0.5)	62 (3)
TMiC	0.7 (0.2)	1 (0.3)	30 (1)
BuNC	3.7 (0.2)	9 (1)	49 (2)

[b] Data not obtained; spectral change small upon substitution of CH_3CN for $P(OBu)_3$.

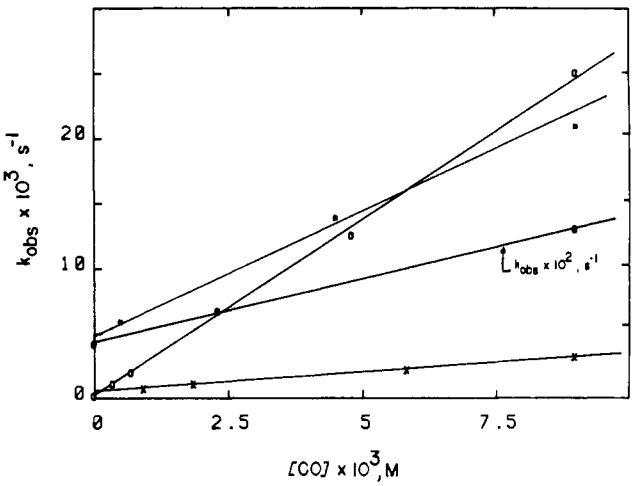

Figure 1. Kinetic data for the reaction $FeN_4(CH_3CN)_2 + CO \rightarrow FeN_4(CH_3CN)CO + CH_3CN$ in CH_3CN at 25 °C for (○) $dmgBF_2$, (●) $bqdBF_2$, (*) $npqBF_2$, and (×) $Me_4[TIM]$. Note for that for $bqdBF_2$, 10^2k_{obs} is plotted.

from the ratio of the forward and reverse rate constants. These values are found to be in good agreement with values obtained from analysis of the visible spectra of equilibrated solutions of the $FeN_4(CH_3CN)_2$ complexes with various concentrations of CO using standard spectrophotometric methods. The exceptionally high value of the binding constant for the dmg system requires only very low CO concentrations (10^{-4} M) in order to achieve appreciable binding even in neat CH_3CN. Typical plots of k_{obs} vs [E] for reaction 5 are given in Figure 2 for the dmg system. Reactions with CO, TMIC, and $P(OBu)_3$ go to completion and give zero intercepts. The reaction with pyridine gives a nonzero intercept consistent with an approach to equilibrium and affords the value of k_{-py}^{A}. Spectrophotometric titration of $FeN_4(CH_3CN)_2$ with pyridine in acetonitrile shows two distinct spectral changes from which approximate values of the stepwise equilibrium constants are obtained. The spectrophotometrically derived constant $K_{A,py}^{A}$ is in good agreement with that obtained from the ratio of the slope to the intercept of the kinetic plot for py in Figure 2. The rates for the second step (reaction 6) are substantially slower than those for the first, consistent with the well-known trans-

(18) Reactions at 0.4 M MeIm proceed with clean isosbestic points with no detectable formation of either $Fe(dioxBF_2)_2(MeIm)(CO)$ or $Fe(dioxBF_2)_2(MeIm)(CH_3CN)$. In addition for the bqd and npq cases replacement of CO by CH_3CN proceeds at the same rate as reaction 9.

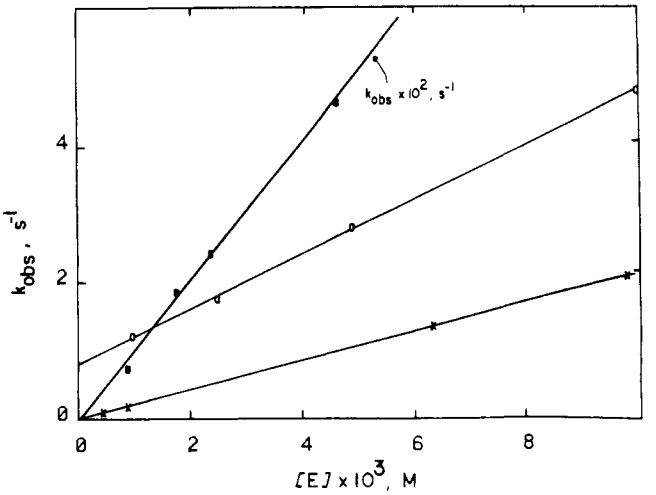

Figure 2. Kinetic data for the reactions $Fe(dmgBF_2)_2(CH_3CN)_2 + E \rightarrow Fe(dmgBF_2)_2(CH_3CN)E + CH_3CN$ in CH_3CN at 25 °C (E = (●) $P(OBu)_3$, (○) py, (×) TMIC). Note for E = $P(OBu)_3$, 10^2k_{obs} is plotted.

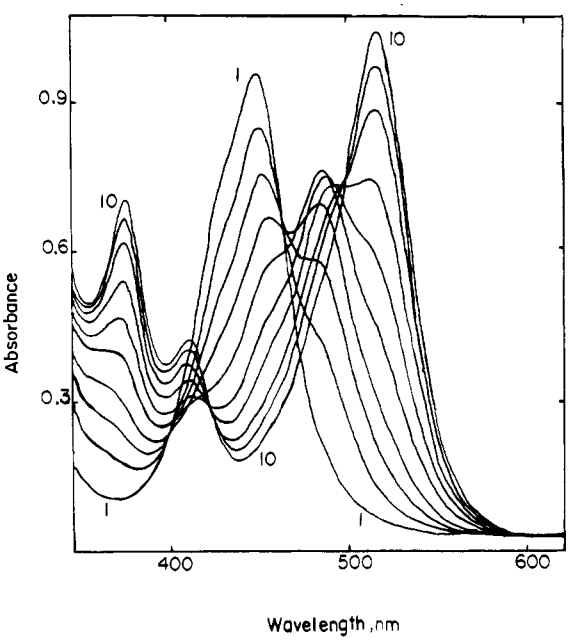

Figure 3. Spectrophotometric data for titration of $Fe(dmgBF_2)_2(CH_3CN)_2$ with py. Data are at 25 °C in N_2-purged CH_3CN with [py] = 0, 0.4, 1.01, 2.00, 3.94, 7.6, 15.3, 34.6, 75.7, and 660 mM in spectra 1–10, respectively.

Table VI. Kinetic and Equilibrium Data[a] for Py Binding to $FeN_4(CH_3CN)_2$ Complexes in CH_3CN at 25 °C

	Fe-$(dmgBF_2)_2$	Fe-$(bqdBF_2)_2$	Fe-$(bqdBF_2)_2$	Fe$(Me_4$-[TIM]$[^{2+}$
$FeN_4(CH_3CN)_2 + py \rightleftharpoons FeN_4(CH_3CN)py + CH_3CN$				
$10^{-4}K_{A,py}^{A}$	1 (0.5)	3 (1)	6 (2)	0.1 (0.03)
$10^{-3}k_{-A}^{A}(k_{+py}^{A}/k_{+A}^{A})$, s^{-1}	7.7 (0.4)	1.18 (0.06)		
k_{-py}^{A}, s^{-1}	0.8 (0.03)	0.036 (0.002)		
$FeN_4(CH_3CN)py + py \rightleftharpoons FeN_4(py)_2 + CH_3CN$				
$10^{-3}K_{A,py}^{py}$	1.4 (0.4)	6 (2)	8.5 (3)	
$10^{-3}k_{-A}^{py}(k_{+py}^{A}/k_{+A}^{py})$, s^{-1}	1.2 (0.1)	1.81 (0.08)[d]		
k_{-py}^{py}, s^{-1}	1.1 (0.1)			

[a] From spectral titration unless otherwise indicated. [b] Calculated from kinetic data shown.

delabilizing effect of the π-acceptor ligands. Kinetic data for the reaction

$$Fe(dmgBF_2)(py)(CH_3CN) + py \rightarrow Fe(dmgBF_2)_2(py)_2 + CH_3CN \quad (10)$$

were obtained by a flash-photolysis method,[19] since the reaction

Table VII. Rate Constants[a] for the Dissociation of L Trans to T for $Fe(dioxBF_2)_2TL$ Complexes in Toluene

	$10^3k_{-L}^T$, s^{-1}			$10^3k_{-L}^T$, s^{-1}		
	T, °C	$Fe(dmgBF_2)_2TL$	$Fe(dmgH)_2TL$[b]	T, °C	$Fe(npqBF_2)_2TL$	$Fe(npqH)_2TL$[c]
k_{-N}^N	25	3.3[d]	6.2	25	0.37	1.7
k_{-py}^{py}	10	43	87	25	90	70
k_{-py}^{PO}	45	6.9	1.2	25	0.098	0.028
k_{-CO}^{py}	60	6.4	2.0	25	1.4	1.9

[a] Estimated error ±5%. [b] Reference 3b. [c] Reference 3c. [d] Solvent in CH_2Cl_2.

is complete on mixing at the higher concentrations of py required to drive the reaction to the right. These data are collected in Table VI.

Reactions in Toluene. In order to evaluate the effect of BF_2 substitution on the reactivity of the FeN_4 systems, some reactions of MeIm and py complexes that have direct analogues in the $Fe(dioxH)_2$ systems were studied in toluene solution. These reactions were remarkably similar to the previously reported reactions of their $Fe(dioxH)_2$ analogues.[3] With a large excess of entering ligand, limiting dissociative rate constants that are independent of the concentration and nature of the entering group are obtained. Table VII compares some representative rate constants for the dmg and npq systems involving CO, py, and MeIm dissociation. The trans-delabilizing effects in the two systems are compared in terms of k_{-py}^{PO}. The BF_2 substitution is seen to have only a small effect on the rates of ligand substitution reactions.

Reactions of the $Fe(dmgBF_2)_2(py)_2$ complex with CO, $P(OBu)_3$, and TMIC were investigated in toluene solution at 10 °C to fully establish the D mechanism for this system and to provide values of the ratio k_{+E}^{py}/k_{+py}^{py}. Under pseudo-first-order conditions in both py and entering ligand E, k_{obs} is given by eq 11 A reciprocal

$$k_{obs} = k_{-py}^{py}k_{+E}^{py}[E]/(k_{+py}^{py}[py] + k_{+E}^{py}[E]) \quad (11)$$

plot of the data is given in Figure 4 showing a common intercept identified with $1/k_{-py}^{py}$ and differing slopes reflecting the relative ability of E to compete with py for the pentacoordinate intermediate $Fe(dmgBF_2)_2(py)$. The reverse reaction for the case E = CH_3CN was also investigated by a flash-photolysis method at 25 °C, and the data are also shown in Figure 4. In this case the intercept corresponds to $1/k_{-A}^{py}$ (7.7×10^{-2} s) for trans to pyridine. Values of k_{+py}^{py}/k_{+E}^{py} are 13 (±2), 0.66 (±0.03), 8.7 (±4), and 2.5 (±0.5) for E = CO, TMIC, $P(OBu_3)$, and CH_3CN, respectively.

Kinetic studies of reactions of the $Fe(dioxBF_2)(CH_3CN)_2$ complexes were also carried out in toluene containing 0.001–0.03 M [CH_3CN]. For the reaction with CO at 1 atm of CO, the pseudo-first-order rate constant showed an inverse first-order dependence on [CH_3CN]. Linear plots of k_{obs} vs [CO]/[CH_3CN] gave slopes[20] of 11, 8, and 40 s^{-1} for the dmg, npq, and bqd systems, respectively. These values are consistently about 5 times smaller than the corresponding constants in acetonitrile solution given in Table IV. For the $Fe(dmgBF_2)(CH_3CN)_2$ complex, spectrophotometric titration with pyridine at 1 M [CH_3CN] in toluene affords $K_{A,py}^A = 2.6 \times 10^4$ and $K_{A,py}^{py} = 120$, and kinetic studies of reactions 4 for E = py give values of $k_{-A}^A k_{+py}^A/k_{+A}^A = 1.5 \times 10^4$ s^{-1} and $k_{-py}^A = 0.5$ s^{-1} from experiments exactly analogous to those described above in neat acetonitrile. Kinetic investigations below 0.0001 M [CH_3CN] in toluene were complicated by transients associated with base-off effects or water coordination. The above results are fully consistent with a D mechanism for CH_3CN replacement in toluene and show a pattern

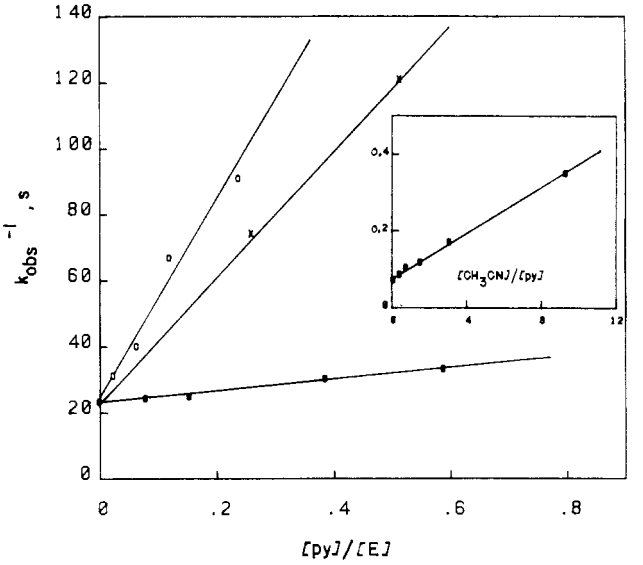

Figure 4. Reciprocal plots for the reaction $Fe(dmgBF_2)_2(py)_2 + E \rightarrow Fe(dmgBF_2)_2(py)E + py$ in toluene at 10 °C (E = (○) CO ([CO] = 7.4 mM), (×) $P(OBu)_3$ ([$P(OBu)_3$] = 0.12 M), (●) TMIC ([TMIC] = 5–15 mM, [py] = 0.4–43 mM). Inset: Reciprocal plot for the reaction $Fe(dmgBF_2)_2(py)(CH_3CN) + py \rightarrow Fe(dmgBF_2)_2(py)_2 + CH_3CN$ in toluene at 25 °C ([py] = 5–33 mM, [CH_3CN] = 3.6–302 mM).

of reactivity fundamentally the same as that found in acetonitrile with small differences associated with solvent effects and with an activity of CH_3CN in neat acetonitrile somewhat less than 19.2 M but greater than 1.0 M.

Discussion

The reactions of the $Fe(dioxBF_2)_2$ complexes are remarkably similar to the corresponding $Fe(dioxH)_2$ analogues. The $Fe(dioxBF_2)_2(CH_3CN)_2$ complexes are about 1000 times more labile than the bis(pyridine) complexes and as a result have substantially greater CO binding constants. In comparison with +2-charged $FeN_4(CH_3CN)_2$ complexes given in Table IV, the $Fe(dioxBF_2)_2$ systems are 1 order of magnitude more labile. The $Fe(dmgBF_2)_2(CH_3CN)_2$ has the highest CO affinity of the systems considered, and the equilibrium for CO binding can be dramatically shifted to the right by going to conditions of low [CH_3CN] to noncoordinating solvents such as toluene or chloroform. The relative CO binding constants and CO lability dmg > npq > bqd are largely the same as found for the dioxH systems. In addition, the relative labilities of CH_3CN, bqd > dmg > npq, inferred from the data in Tables V and VI are similar to previous observations of py and MeIm labilities in dioxH systems in toluene.

The dependence of the rates on the nature and concentration of the entering group is fully consistent with the assumed D mechanism. In acetonitrile, it is impossible to extract the values of the relative rates of addition of CH_3CN and E to the pentacoordinate intermediate. However, if the rate constants in Table V for each system are divided by the value for E = CO, one obtains the discrimination ratios, which are identical with k_{+E}/k_{+CO} if the well-established D mechanism in toluene is assumed for acetonitrile solution. These discrimination ratios are given in Table VIII along with the corresponding numbers obtained in toluene solution from direct competition measurements for $Fe(dmgH)_2MeIm$ reported previously and for $Fe(dmgBF_2)_2py$ and $Fe(dmgBF_2)_2CH_3CN$ derived from kinetic measurements in

(19) A sample of $Fe(dmgBF_2)_2py(CO)$ was photolyzed in nitrogen-purged acetonitrile at [py] = 0.01–0.2 M. Under these conditions the pentacoordinate $Fe(dmgBF_2)_2py$ is efficiently trapped as $Fe(dmgBF_2)_2py(CH_3CN)$, whose subsequent reaction with py is monitored at 480 and 518 nm.

(20) The slopes correspond to $k_{-A}k_{+CO}/k_{+A}$. For the $Fe(dmgBF_2)$ system, the reaction was investigated at higher [CH_3CN] where linearity is lost. For [CH_3CN] = 0.13, 0.52, 0.97, 9.6, and 16 M, k_{obs} = 0.57, 0.17, 0.12, 0.032, and 0.025 s^{-1}. (CO solubility is assumed to be proportional to volume % of toluene and CH_3CN).

Table VIII. Discrimination Ratios[a] Relative to CO in CH_3CN and Toluene for Various FeN_4T Intermediates

intermediate	k_{+CO}/k_{+CO}	k_{+PO}/k_{+CO}	k_{+TMIC}/k_{+CO}	k_{+BuNC}/k_{+CO}	k_{+py}/k_{+CO}
		CH_3CN Solvent			
$Fe(dmgBF_2)_2CH_3CN$	1	4	77	170	150
$Fe(npqBF_2)_2CH_3CN$	1	10	13	27	35
$Fe(bqdBF_2)_2CH_3CN$	1	22	40	>50	
$Fe(Me_4[TIM])CH_3CN^{2+}$	1		19	22	
		Toluene Solvent			
$Fe(dmgH)_2MeIm$[b]	1	1.4 (2)	15 (3)		8 (1)
$Fe(dmgBF_2)_2py$	1	1.5 (1)	26 (5)		15 (2)
$Fe(dmgBF_2)_2CH_3CN$	1		700 (100)		1300 (150)

[a] Obtained from the ratio of rate constants in Table V. [b] Reference 3b.

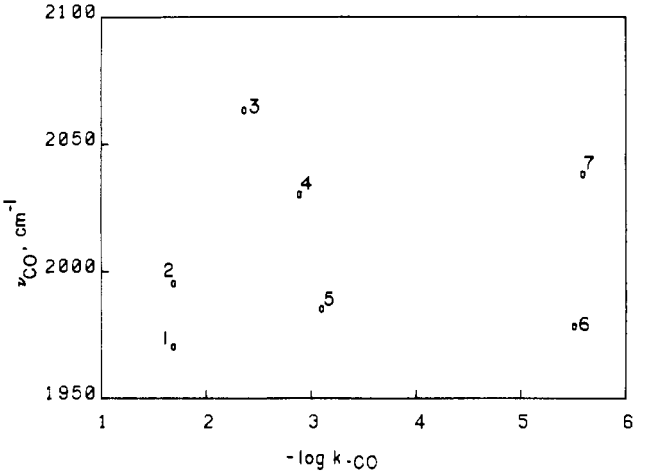

Figure 5. CO stretching frequency vs rate constants for CO dissociation at 25 °C for (1) $Fe(dmgH)_2(MeIm)CO$,[3b] (2) Fe(PpIX)(py)CO,[17,26] (3) $Fe([14]aneN_4)(CH_3CN)CO^{2+}$,[5a] (4) $Fe(Me_4[TIM])(MeIm)CO^{2+}$,[5b] (5)$Fe(dmgBF_2)_2(py)CO$, (6) $Fe(npqBF_2)(py)CO$, (7) Fe(Pc)(py)CO,[5g] and (8) $Fe(bpdBF_2)_2(CH_3CN)CO$.

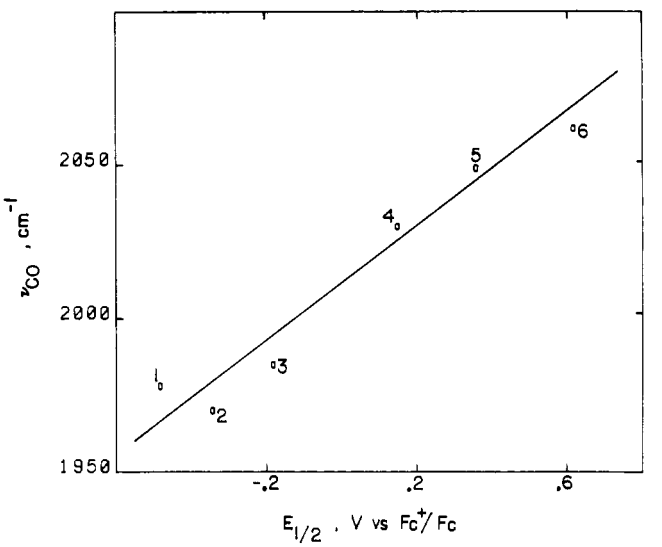

Figure 6. Correlation of ν_{CO} for $FeN_4(L)CO$ with $E_{1/2}$ for FeN_4L_2: (1) $Fe(dmgH)(MeIm)$;[3b] (2) Fe(PpIX)(py);[17,27] (3) $Fe([14]aneN_4)(CH_3CN)^{2+}$;[5a,17] (4) $Fe(Me_4[TIM])(MeIm)^{2+}$;[5d,5h] (5) $Fe(dmgBF_2)_2(py)$; (6) $Fe(npqBF_2)_2(CH_3CN)$.

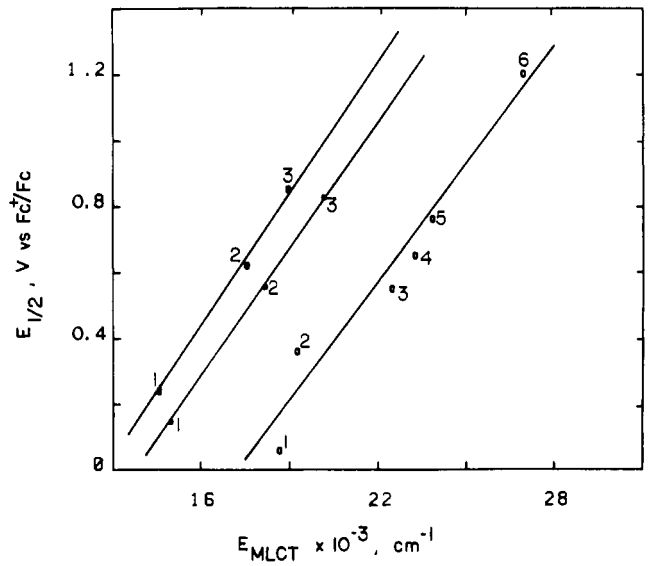

Figure 7. Correlation of $E_{1/2}$ with energy of MLCT for FeN_4TL (N_4 = (O) $Fe(dmgBF_2)_2TL$ (T, L = (1) MeIm, MeIm, (2) py, py, (3) CH_3CN, CH_3CN, (4) CH_3CN, BuNC, (5) CH_3CN, TMIC, (6) CH_3CN, CO), (*) $Fe(Me_4[TIM])TL^{2+}$ (T, L = (1) MeIm, MeIm, (2) CH_3CN, CH_3CN, (3) CH_3CN, TMIC), (●) $Fe(npqBF_2)_2TL$ (T, L = (1) MeIm, MeIm, (2) CH_3CN, CH_3CN, (3) CH_3CN, TMIC) complexes.

toluene obtained in this work. Similar trends are found in all systems (CO is the slowest, RNC and py the greatest), and these trends parallel directly determined on-rate constants for hemes.[3b] The values for $Fe(dmgBF_2)_2CH_3CN$ are seen to span a larger range than those for the other systems shown, but this greater discriminating ability is not found in toluene when py is the fifth ligand.

Correlations of Kinetic, Redox, and Spectroscopic Data. The electronic effect of BF_2 substitution in $Fe(dioxH)_2$ systems is seen to be great on the CO stretching frequencies, redox potentials, and air stabilities of the complexes but remarkably small on MLCT energies and rates of ligand substitution reactions. These results are consistent with BF_2 exerting a global σ-electron-withdrawing effect that lowers the energy of the HOMO ($d_{xz,yz}$) as well as that of the dioxime π^* level. This would explain the lowering of the redox potential while the MLCT energy remains almost unchanged. The very small effect of BF_2 on the rates of ligand dissociation is somewhat surprising, especially for loss of CO in view of the marked shift in the CO stretching frequency. From previous studies on $Fe(dioxH)_2$ systems, it is clear that π-bonding effects play an important role in rates of axial substitution reactions. The conventional explanation for the inertness of low-spin d^6 systems is that the d-orbital stabilization energy is lost along the reaction coordinate for ligand dissociation. It is important perhaps to note that the stabilization of $d_{xz,yz}$ arising from the global σ stabilization of BF_2 is not altered along the reaction coordinate for axial ligand dissociation and therefore does not contribute to the barrier. This result is of some importance because it suggests that the σ-donor properties of the cis N_4 ligand may have only a small effect on the lability of the axial ligands. If true, then the unusual lability differences of FeN_4 systems must be due to π-bonding or other effects.

The remarkable differences in the effects of BF_2 on various properties of the iron complexes challenge our understanding of the origins of correlations between spectroscopic, redox, and rate parameters often described in the literature. For example it is often erroneously assumed that CO stretching frequencies correlate with metal–CO bond strengths. Data for a variety of $FeN_4L(CO)$ systems are plotted in Figure 5. The dissociative rate constant for CO loss from these systems in an excellent measure of the

relative Fe–CO bond energies,[21] yet there is no correlation at all with the CO stretching frequencies. In fact the CO stretching frequencies correlate much better with redox potentials, as seen in Figure 6. Morse[22] and Morris[23] have previously found such a correlation for a wide variety of organometallic compounds. We have previously discussed the deceptively simple notion of metal–ligand bond energies in highly covalent synergistic bonding situations.[24] A careful analysis shows that dissociation of CO or MeIm in $FeN_4(MeIm)(CO)$ results in substantial changes in the bond strength of the remaining axial ligand. These changes in the bonds not broken contribute to the kinetic barrier associated with k_{-L}. When a CO bond is stretched slightly, it is unlikely that the other iron–ligand bonds are significantly perturbed. Thus, there are significant energetic factors associated with the Fe–CO bond energy that have no corresponding component in the CO stretching frequency.

While $E_{1/2}$ does not correlate with the MLCT energy for different N_4 ligands, within a given N_4 system, an excellent correlation between $E_{1/2}$ and E_{MLCT} is observed as shown in Figure 7.[25] The slopes of the plots are nearly 1.0 (when identical units are used for both axes), consistent with both $E_{1/2}$ and E_{MLCT} benefitting from the stabilizing of $d_{xz,yz}$ by π-acceptor ligands. It should be noted that rate data and $E_{1/2}$ are correlated in the increasing trans destabilization of MeIm or py in $Fe(dmgH)_2TL$ complexes,[3] the trans effects of anation rates of $Ru(NH_3)_4T-(H_2O)^{2+}$ systems,[26] and perhaps the lability of CH_3CN and MeIm in various $FeR_4[TIM]^{2+}$ systems.[5d]

Acknowledgment. We thank A. B. P. Lever for use of the electrochemical equipment and Philip Lefko for his contributions in the preliminary phase of this work. Support of the Natural Sciences and Engineering Research Council of Canada is gratefully acknowledged.

(21) Tsou, T. T.; Loots, M.; Halpern, J. *J. Am. Chem. Soc.* **1982**, *104*, 623.
(22) Cook, R. L.; Morse, J. G. *Inorg. Chem.* **1984**, *23*, 2332.
(23) Morris, R. H.; Earl, K. A.; Luck, R. L.; Lazarowych, N. J.; Sella, A. *Inorg. Chem.* **1987**, *26*, 2674.
(24) Stynes, D. V.; Fletcher, D.; Chen, X. *Inorg. Chem.* **1986**, *25*, 3483.
(25) (a) Dodsworth, E. S.; Lever, A. B. P. *Chem. Phys. Lett.* **1985**, *119*, 61. (b) Lever, A. B. P. *Inorg. Chem.* **1990**, *1271*, 29.
(26) Franco, D. W.; Taube, H. *Inorg. Chem.* **1978**, *17*, 571. Isied, S. S.; Taube, H. *Inorg. Chem.* **1976**, *15*, 3070.

Contribution from the Department of Chemistry, Washington State University, Pullman, Washington 99164-4630

Solvent Dependence of the Electron Self-Exchange of Hexakis(2,6-diisopropylphenyl isocyanide)chromium(0,I) and -chromium(I,II) and a Comparison with Theoretical Models

Kim A. Anderson and Scot Wherland*

Received January 26, 1990

The rate of electron self-exchange between chromium(I) hexakis(2,6-diisopropylphenyl isocyanide) tetrafluoroborate, $Cr(CNdipp)_6BF_4$, and $Cr(CNdipp)_6(BF_4)_2$ has been measured as a function of reactant concentration, temperature, and solvent (acetone, acetonitrile, nitromethane, methylene chloride, methanol) by ^1H NMR line broadening. The rate of electron self-exchange between $Cr(CNdipp)_6$ and $Cr(CNdipp)_6BF_4$ has been measured as a function of temperature in acetone. The Cr(0)/Cr(I) rate constants, ca. 10^8 M^{-1} s^{-1}, are a factor of 10 higher than the Cr(I)/Cr(II) values in methylene chloride and acetone. The Cr(I)/Cr(II) rate constants vary little between the solvents at 298 K. The activation parameters do vary, showing a compensating pattern for the solvents studied. The results for the two systems are compared with the predictions of the standard Marcus collision and solvent dynamic models. The experimental electron self-exchange rate constants are in excellent agreement and the activation parameters are in reasonable agreement with the predictions from the Marcus collision model. The calculated activation parameters from the Marcus collision model show no trend with solvent, and thus do not predict the compensation behavior.

Introduction

Outer-sphere electron self-exchange reactions are of particular interest in the field of mechanistic inorganic chemistry because the electron self-exchange rate constant is characteristic of an oxidation–reduction couple, analogous to a reduction potential. Furthermore, theoretical treatment of these reactions is simpler than the treatment of electron-transfer cross-reactions, which involve net chemical change.[1-5] As part of our ongoing effort to study nonaqueous electron transfer by transition-metal complexes, we have chosen the Cr(O,I,II) hexakis(2,6-diisopropylphenyl isocyanide), $Cr(CNdipp)_6^{0/+}$ and $Cr(CNdipp)_6^{+/2+}$, systems for detailed study. Several features of this class of complexes make them appealing. They are substitution inert in three oxidation states (Cr(O,I,II)), X-ray crystal structures have been determined for four oxidation states (Cr(O,I,II,III)) of $Cr(CNC_6H_5)_6$,[6] a variety of analogous symmetrical complexes with other isocyanide ligands can be synthesized, they have adequate stability and solubility in nonaqueous solvents over a large temperature range, and electron self-exchange can be followed directly by ^1H NMR line broadening.[6-8]

The two couples, $Cr(CNdipp)_6^{0/+}$ and $Cr(CNdipp)_6^{+/2+}$, are identical, having the same metal ion and ligand set, except for charge. In the former the reactants are neutral and singly charged; therefore, there is no Coulombic work term contributing to the electron-transfer rate. In the latter system both reactants are charged and there is Coulombic repulsion between the reactants.

(1) Marcus, R. A.; Sutin, N. *Biochim. Biophys. Acta* **1985**, *811*, 265.
(2) Newton, M. D.; Sutin, N. *Annu. Rev. Phys. Chem.* **1984**, *35*, 437.
(3) Nielson, R. M.; McManis, G. E.; Golovin, M. N.; Weaver, M. J. *J. Phys. Chem.* **1988**, *92*, 3441. Farina, R.; Wilkins, R. G. *Inorg. Chem.* **1986**, *7*, 514. Krishnam, C. V.; Cruetz, C.; Schwarz, H. A.; Sutin, N. *J. Am. Chem. Soc.* **1983**, *105*, 5617.
(4) Brunschwig, B. S.; Logan, J.; Newton, M. D.; Sutin, N. *J. Am. Chem. Soc.* **1980**, *102*, 5798.
(5) Guarr, T.; McLendon, G. *Coord. Chem. Rev.* **1985**, *68*, 1.
(6) Bohling, D. A.; Mann, K. R. *Inorg. Chem.* **1984**, *23*, 1426.
(7) Essenmacher, G. J.; Treichel, P. M. *Inorg. Chem.* **1977**, *16*, 800. Weber, W. P.; Gokel, G. W. *Tetrahedron Lett.* **1977**, *17*, 1637.
(8) Anderson, K. A.; Wherland, S. *Inorg. Chem.* **1989**, *3*, 601.

0020-1669/90/1329-3822$02.50/0